Volume 21, No 1 | International Journal of Radiation Research, January 2023

Simulation based analysis of ^{4}He, ^{7}Li, ^{8}Be and ^{10}B ions for heavy ion therapy

F. Ekinci[1*], E. Bostanci[2], M.S. Güzel[2], O. Dagli[3]

[1]*Ankara University, Institute of Nuclear Sciences, Besevler 10. Yıl Campus, Tandogan Ankara, Turkey*
[2]*Ankara University, Computer Engineering Department, Golbasi, Ankara, Turkey*
[3]*Gazi University, Faculty of Medicine, Department of Neurosurgery Gamma Knife Unit, Ankara, Turkey*

► ***Original article***

Corresponding author:
Fatih Ekinci, Ph.D.,
E-mail:
fatih.ekinci@hotmail.com.tr

Received: April 2022
Final revised: October 2022
Accepted: November 2022

Int. J. Radiat. Res., January 2023; 21(1): 131-137

DOI: 10.52547/ijrr.21.1.18

Keywords: *Heavy ion therapy, Bragg cure, recoil, lateral straggle, phonon.*

ABSTRACT

***Background*:** The therapeutic usage of heavy ions has received much attention due to its advantageous physical and radiobiological assets compared to photon-based therapy. Thanks to these unique properties of heavy ion radiotherapy, it can allow dose increase in tumors while reducing the radiation dose in adjacent normal tissues. ***Materials and Methods*:** The main aim of this study is to analyze the LET, recoils, lateral scattering, and phonon energies of selected ^{4}He, ^{7}Li, ^{8}Be and ^{10}B heavy ions in the water phantom in the therapeutic energy range. This analysis was performed by using MC based TRIM simulation method of interactions. ***Results*:** The main innovation that this study will provide to the literature is not only ionization but also the calculation of recoils, lateral scattering and phonon oscillation resulting from all interactions. According to the calculation results, the largest recoils peak value was found to be 7.957 eV/A-ion×10^{3} in the B ion, and it was observed that it formed an average of 88% more recoil peaks than He ion, 53% on average than Li ion and 24% more than Be ion on average. In the lateral scattering, the greatest value occurred in the He ion. It should be noted that He ion produced 42%, 57% and 71% more lateral scattering than Li, Be and B ions respectively. As a result of all these interactions, 32% of the phonon and 68% of the phonon were formed respectively by the recoil interactions. ***Conclusion*:** This study includes ionization and all particle-based target interactions.

INTRODUCTION

The therapeutic advantages of heavy ion therapy were primarily introduced by Robert Wilson at the beginning of 1940s [1, 2]. Heavy ion beams gathered lots of attention from radiation oncology more than 60 years because of their superior physical and biological advantages over well-known high-energy photon beams [3]. Protons are currently used in more than 61 facilities worldwide [4]. There are "16" centers in clinical operation in Europe. Based on the outstanding clinical results obtained via carbon ion beams in Japan, several carbon ion therapy centers have been started in Europe within the previous decade. Lately, researchers have also concentrated on particle types other than protons and carbon ions, ionization interactions of helium and oxygen ions [5,6]. The clinical success of heavy ion therapy depends on various clinical aspects as well as dosimetric accuracy, comprising accurate dose calculations and beam delivery, correspondingly. Until now, most of the clinical experience in particle beam therapy has been gained with radiotherapy treatment planning and dose calculations using semi-analytical pen beam methods [7, 8].

Besides the extensive clinical experience gathered worldwide with heavy ion beams such as proton and carbon, other heavy ions may be considered as future treatment options. Radiotherapy with these different heavy ions marks a new era in the field of high-sensitivity cancer therapy [9]. Comparative studies using several types of heavy ions need to be evaluated with a new treatment plan to identify patients who benefit most from this technologically demanding treatment [9].

In each new heavy ion treatment plant, the selection of ion species and their energies depend on the Linear Energy Transfer (LET) and ionization interactions of the ions in question [10]. Thus, the properties of different heavy ions such as ^{1}H, ^{4}He, ^{6,7}Li, ^{8}Be, ^{10}B, ^{12}C, ^{14}N and ^{16}O at therapeutic energies, such as dose, LET, and ionization, were investigated by the MC method [11,12]. In addition, the depth dose distributions, lateral scattering and Bragg peaks of heavy ions in Heidelberg Ion Therapy Center (HIT) were investigated experimentally [13]. For range estimation during or after irradiation of heavy ions, studies are underway to view the beam LET and position of irradiated heavy ions, especially with respect to the depth in the measurement phantom

[DOI: 10.52547/ijrr.21.1.18]

[14]. However, it has been observed that there is not enough research in the literature on the lateral scattering, backscattering, and phonon energies of these ions within the target at therapeutic energy. These deficiencies caused that all interactions of the heavy ion to be selected within the target could not be fully revealed. Moreover, to overcome the real *in-vivo* LET distribution uncertainties and the biological effects of different radiation characteristics, research should be validated by using reliable and high-throughput simulation programs.

The most widely used of these simulation programs are Monte Carlo (MC) based systems. It should be noted that in the absence of an experimental heavy ion beam line, MC-based simulations are the most accurate way to establish reference values [15]. The development of innovative approaches for biophysical dosimetry and the definition of robust criteria are essential to ensure that new clinically available cancer particle therapies are of high quality [16]. In line with this goal, it is particularly important in the experimental validation of data by mimicking biological experiments with simulations. These calculations, aimed in this study, were obtained with MC systematics. General purpose MC codes are considered the "gold standard" for accurate calculation of dose in target material [17]. One of these simulation systems, "Stopping and Range of Ions in Matter (SRIM)", is a software tool developed by "Ziegler (Rockville, MD, USA)" based on the "Binary Collision Approach (BCA)" method [18]. SRIM can calculate many possibilities regarding the movement of ions in matter [18-22]. BCA is an MC method designed to calculate deposition profiles in materials exposed to energetic ion beams can be seen in [18-22]. The basic principle in this method is that an energetic particle loses its kinetic energy because of collision with a target atom [19]. This energy loss is defined as the energy transferred by ions to target atoms by considering elastic and inelastic collisions with electrons [18-22].

In this study, ionization, recoils, phonon and lateral scattering values of helium, lithium, beryllium, and boron ions formed by water phantom were calculated with the help of MC (Markov approach) Transport of Ions in Matter (TRIM) (Sandia Laboratories, Livermore, California, U.S.A.) simulation program. In these calculations, data obtained for each selected heavy ion were compared with each other. First, in these comparisons, it was tried to determine the ion that creates the most LET energy. Then the ion generating the lowest recoils and photon energy was determined. Finally, it is aimed to determine from which heavy ion the least lateral scattering value comes from. The main innovation of this study is to examine the phonon interactions resulting from recoils and primary and secondary interactions. In particular, the contribution of atoms detached from both the bullet ion and the target crystal structure to the total LET because of recoil interactions occurring in the crystal structure was investigated. Thus, not only ionization-induced interactions, but also recoils and phonon-based interactions were revealed.

MATERIAL AND METHOD

MC TRIM

TRIM is one of the critical SRIM modules extensively employed in ion beam implantation and processing designs [22]. TRIM has the ability to analyze interaction in complex targets (Compound materials), also offering different options for assessing destruction to a target, depending on the type and details of outputs required. The full damage rank (F-C) mod can observe every recoil atoms, involving Primary, secondary, etc., till its energy drops below the "displacement threshold energy (E_d)" of any target atom. Consequently, all targeted collisions can be examined. Quick damage calculation (K-P) mode can only follow the path of arrival of ions, can be used when little attention is required to details of target damage or surface spraying. The damage calculated using this option is a simple statistical method designed on the "Kinchin-Pease formalism (K-P)" [21]. Both F-C and K-P options provide the same ion ranges in each target [20]; nevertheless, compared to the K-P method, the first one requires a long time since the progression of the cascade is not followed. Since we are focusing on the spacing of the ions and the depth of the damage rather than the details of damage. It should be noted that the second method was adopted in this study. The "K-P" theory was initially introduced by Kinchin and Pease. The theory was improved by Lindhard and then employed by Norgett, Robinson and Torrens (NRT) (26). In this theory, the energy E_v is derived from the transferred energy T of the recoil (can be seen in eq. 1), considering the electronic losses [18]:

$$E_v = \frac{T}{1+K_d g(\varepsilon_d)} \quad (1)$$

Where; the electronic losses (See Eq. 2) are governed by:

$$K_d = -0.1334 Z_2^{2/3} M_2^{-1/2} \quad (2)$$

Where; Z_2 and M_2 represent the atomic number and mass (can be seen in eq. 3) for the target atoms and:

$$g(\varepsilon_d) = \varepsilon_d + 0.40244 \varepsilon_d^{3/4} + 3.4008 \varepsilon_d^{1/6} \quad (3)$$

Where; ε_d is a reduced energy (see eq. 4) given by:

$$\varepsilon_d = 0.01014 Z_2^{7/3} T \quad (4)$$

from the transferred energy to target atoms, "E_v", the displacements, "ν", is calculated by using the modified "Kinchin-Pease model" (can be seen in equations 5-6):

[DOI: 10.52547/ijrr.21.1.18]

$$v = 1, if\ E_d < E_v < 2.5E_d \quad (5)$$

$$v = \frac{0.8E_v}{2E_d}, if\ E_v > 2.5E_d \quad (6)$$

Displacement energy is the energy that a recoil atom needs to handle the lattice forces and move more than one atom from its original position. Lattice binding energy, on the other hand, allows each target atom loses when it exits the lattice region and rebounds on the target, and surface binding energy is the energy that the target atoms must handle to leave the target's surface [24].

The second interaction, lateral scattering, is an important concept in this study. Heavily charged particles do not travel in a perfectly straight direction through the target. Deflections in the ion beam direction occur due to ionization, atomic-size collisions, and recoils. This is where the important concept of lateral scattering emerges. Lateral scattering is a measure of the amount of scattering from the direction of each ion in the target. Lateral scattering occurs mostly at the Bragg peak point [25]. So, the scattering is defined as:

$$\sigma = [\ (\Sigma_i x_i^2) / N - R_y^2\ ]^{1/2} = <(\Delta x_i)^2>^{1/2} \quad (7)$$

Shown in equation 7 x_i is the projection range of ion i on the X-axis, that is, the vertical distance of an ion's trace from the surface to the endpoint. $\Sigma_i x_i$ is the sum of ion projection ranges; $\Sigma_i x_i / N$ is the mean projection range of N ions and <x> is the average projection range of all ions. R_y is the lateral projection range. The transverse coordinate y is treated in the same way and only the distance in the XY plane is considered [25]). Therefore, the average lateral projection range is zero ($R_y = 0$). Moreover, the ranges predicted by Y and Z are averaged to increase statistical accuracy [25]. As given in the Lateral Straggle equation 8:

$$\sigma_y = [\ \Sigma_i ((|y_i| + |z_i|)/2)^2 / N\ ]^{1/2} \quad (8)$$

Phantom

By considering the current approach, a water phantom was employed to confirm patient radiotherapy plans for heavy ion therapy [25]. An attempt was made to accurately administer the dose and calibrate the target tissue using a water phantom [24]. This is an essential process since one of the important problems for radiotherapy is whether the desired dose can be given to the patient correctly. Water is considered the main component of the human body; therefore, water is the most significant medium used in the field of medical physics. Reliability of dose and LET calculations for water and accurate calculation of their distribution is particularly essential [26, 27]. The phantom in figure 1 was formed from these liquid water materials in a volume of 15cm×15cm×15cm and irradiated with ^{4}He, ^{7}Li, ^{8}Be and ^{10}B ions beams. The heavy ion beam was sent to the water phantom from its side surface. In the TRIM simulation program, the atomic percentage, atomic density, and density of water parameters were determined according to the ICRU-276 report [27].

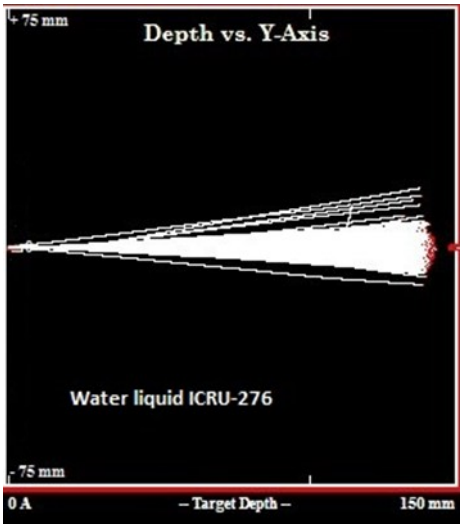

Figure 1. Schematic representation of heavy ion beam and water phantom from MC TRIM simulation program.

Ion beam feature

A heavy ion beam with average of 10^6 particles (general clinical standards: 10^4-10^7 particles) was used in the experiments as used in medical treatment centers. Calculation outputs such as Ion range, sputtered atoms collision details and recoils were selected for analysis. Four different ion beam energies were determined as 80 MeV/u, 100 MeV/u, 120 MeV/u and 140 MeV/u so as to compare the selected heavy ions with each other.

RESULTS

Ionization

The Bragg peak position and amplitude formed by ^{4}He, ^{7}Li, ^{8}Be and ^{10}B heavy ions with 80-140 MeV/u energies are shown in table 1. Average Bragg peak amplitude was calculated as 3.692 eV/A, 4.199 eV/A, 6.816 eV/A, and 10.492 eV/A for He, Li Be and B ions, respectively. As the heavy ion beam energy increases, the Bragg peak position is shifted for all heavy ions, as expected. Besides, as the heavy ion beam energy increases, the Bragg peak amplitude also changes. The range of the heavy ion beam at the phantom is inversely proportional to the Bragg peak amplitude. It was observed that the longest-range value in the selected heavy ion beams occurred in the He ion. The next longest-range values occurred in Li ion. As the energy increased, there were 2.9 cm average range increases for He ion, 2.2 cm for Li ion, 1.7 cm for Be ion and 1.3 cm for B ion, respectively.

[DOI: 10.52547/ijrr.21.1.18]

Table 1. Range (cm) and Bragg peak amplitudes (eV/A) of heavy ion beams in the water phantom.

Ion	80 MeV/u		100 MeV/u		120 MeV/u		140 MeV/u	
	"Range" (cm)	"Peak" (eV/A)	"Range" (cm)	"Peak" (eV/A)	"Range" (cm)	"Peak" (eV/A)	"Range" (cm)	"Peak" (eV/A)
He	**5.1**	**8.572**	**7.7**	**2.351**	**10.5**	**1.928**	**13.8**	**1.915**
Li	4.1	4.065	5.9	3.583	8.3	4.308	10.8	4.255
Be	3.0	7.725	4.4	5.712	6.2	7.715	8.1	6.112
B	2.4	8.157	3.4	12.244	4.8	11.042	6.3	10.525

Reoil

The recoil curves of ^{4}He, ^{7}Li, ^{8}Be and ^{10}B heavy ions with energies of 80-140 MeV/u obtained from this study are shown in figure 2. As it can be seen in tables 1 and 2, while heavy ions lost 99.8% of their energy on average in the water phantom with ionization, they lost 0.02% with recoils. It has been observed that the bullet particle, target atoms, destroying the target crystal structure with the interaction of the recoils, are involved in the interaction. Thus, the recoil interaction is the most crucial factor that changes the direction of the projectile heavy ion and causes deviations in the direction and direction of the progress in the target. These effects are considered critical in the treatment of tumors close to critical points. As depicted in figure 3, the recoil range of heavy ions increases as the beam energy increases and maximum recoil energy occurs at the Bragg peak position. Thus, it is seen and noted that all interactions of the heavy ion beam are at the Bragg peak position.

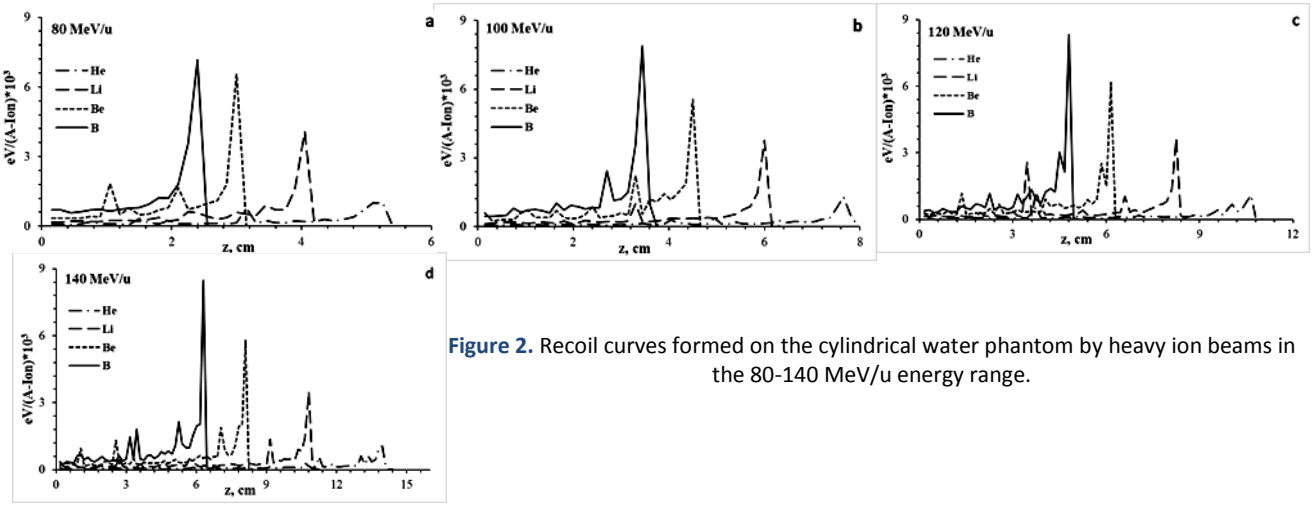

Figure 2. Recoil curves formed on the cylindrical water phantom by heavy ion beams in the 80-140 MeV/u energy range.

The contribution of the atoms removed from the target crystal structure by the atom-to-atom collisions of the bullet ions to the recoil peaks is given in table 2. These contributions were determined by looking at the outputs we received from the TRIM program. The He ion generated an average of 1.114 eV/A-ion×10^{3} recoil peaks at all energies. While the contribution of the H atom to this peak was 37% on average, the contribution of the O atom was 64% on average. Li ion generated an average of 3.746 eV/A-ion×10^{3} recoil peaks at all energies. While the contribution of the H atom to this peak was 37% on average, the contribution of the O atom was 64% on average. The Be ion generated an average of 6.013 eV/A-ion×10^{3} recoil peaks at all energies. While the contribution of the H atom to this peak was 35% on average, the contribution of the O atom was 65% on average. Finally, the B ion generated an average of 7.957 eV/A-ion×10^{3} recoil peaks at all energies. While the contribution of the H atom to this peak was 35% on average, the contribution of the O atom was 65% on average.

Table 2. Recoils peak values (eV/A-Ion×10^{3}) and contributions (%) of H and O atoms forming the water to these values.

Ion	80 MeV/u			100 MeV/u			120 MeV/u			140 MeV/u		
	Recoil Peak	H	O	Recoil Peak	H	O	Recoil Peak	H	O	Recoil Peak	H	O
He	**1.009**	**36**	**64**	**1.307**	**35**	**65**	**1.093**	**39**	**62**	**1.047**	**36**	**64**
Li	4.080	37	63	3.756	34	66	3.656	38	62	3.491	37	63
Be	6.562	35	65	5.547	35	65	6.160	36	64	5.783	33	67
B	7.156	34	66	7.888	33	67	8.317	36	64	8.467	35	65

Phonons

Phonons are generated during and after the interaction of ionization and recoils caused by heavy ion beam in the cylindrical water phantom. The results obtained from the TRIM program are analyzed and the phonon values consisting of ionization and recoils interactions are given in table 3. It was observed that phonon production decreases as the atomic masses of heavy ions increase, and their energies decrease. While the contribution from the ionic interactions to the phonon production formed by the interaction of the He ion was 34% on average,

[DOI: 10.52547/ijrr.21.1.18]

the contribution from the recoil interactions was 66% on average. Respectively, the ionic contribution in Li ion is 32.5% on average, the contribution from recoil interactions is on average 67.5%, the ionic contribution from Be ion is 31.3% on average, the contribution from recoil interactions is 69% on average, and finally, the ionic contribution from B ion is 30.5% on average, the contribution from recoil interactions is 69.5% on average.

Table 3. Phonon values (eV/A×10^3) formed by ion and recoil interactions and percentage contributions.

Ion	80 MeV/u				100 MeV/u				120 MeV/u				140 MeV/u			
	ion		recoil		ion		recoil		ion		recoil		ion		recoil	
	eV/A	%	eV/A	%	eV/A	%	eV/A	%	eV/A	%	eV/A	%	eV/A	%	eV/A	%
He	**0.039**	**33**	**0.080**	**67**	**0.034**	**34**	**0.065**	**66**	**0.028**	**34**	**0.054**	**66**	**0.024**	**35**	**0.046**	**65**
Li	0.091	32	0.197	68	0.071	32	0.149	68	0.061	33	0.125	67	0.052	33	0.106	67
Be	0.153	30	0.350	70	0.124	31	0.275	69	0.104	32	0.224	68	0.090	32	0.191	68
B	0.221	30	0.524	70	0.181	30	0.413	70	0.154	31	0.343	69	0.135	31	0.295	69

Lateral scattering

The lateral scattering values of ^{4}He, ^{7}Li, ^{8}Be and 10B heavy ions in the 80-140 MeV/u energy range are given in figure 3. It was observed that the lateral scattering increased as the energy of the ion beam increased. The main reason for this is that heavy ions reach a greater range in the phantom. Thus, further ionization and atom-to-atom collisions cause heavy ion beams to scatter laterally in their direction of travel. It was observed that there is a relationship between beam energy of heavy ions and lateral scattering in He ion $y = 0.0003x^{1.7388}$, in Li ion $y = 0.0002x^{1.7084}$, in Be ion $y = 0.00006x^{1.8966}$ and in B ion $y = 0.00005x^{1.8489}$. With an energy increase of 20 MeV/u in the energy range of 80-140 MeV/u of the heavy ion beam, the lateral straggle increased by 0.280 mm in He ion, 0.178 mm in Li ion, 0.145 mm in Be ion and 0.089 mm in B ion on average.

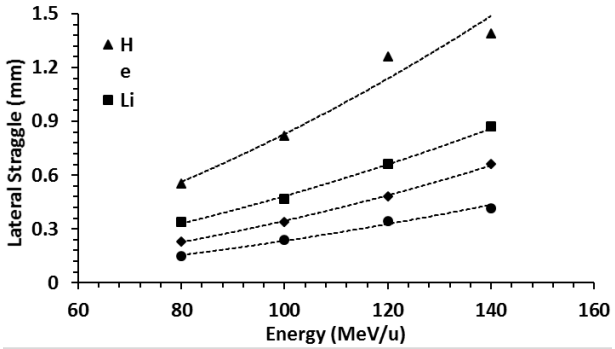

Figure 3. Lateral straggle for 80-140 MeV/u heavy ion beams.

DISCUSSION

It was observed that the recoil value increased as the mass number of heavy ions used in the heavy ion beam increased [28]. Recoils interaction contributed to the Bragg peak value and contributed more photon production than this contribution. Regardless of the ion mass number used, the ion and recoil contribution are the same on average [28]. As the atomic weight of heavy ions increased, ion-derived phonon production decreased, while recoil-induced phonon production increased. The total dose can be increased by using Energy obtained from phonons [28]. This increase may also occur at points further away from the intended point of interaction. This situation can cause damage to healthy tissues as well as a risk of secondary cancer. Lateral scattering is a parameter that should be considered in tumor treatment close to critical tissues. Lateral scattering has been the subject of study in similar studies [13, 28]. It was observed that the lateral scattering values of the same heavy ion beam in different biomaterials increased with the increase of beam energy [28]. A unique feature of particle therapy is the precise dose delivery in the tumor mass with a steep dose gradient that preserves the normal tissues surrounding the cancerous tissue [29]. However, biological efficacy and lateral dose distributions may differ between different particle beams. Based on these differences and tumor characteristics, optimal radiation therapy can be individualized for each cancer patient [29, 30]. As with the data we presented in our study, heavier particles provide a higher level of dose fidelity that improves tumor control while sparing normal tissues and organs at risk [31]. For example, in this study, notable steep lateral scattering was found if Li, Be or B beams were preferred over ^{4}He beams, as suggested in previous studies [32, 33], strengthening its possible future clinical application. As the atomic weight of the ions increases, they exhibit advantageous physical properties [34, 35] and cause less lateral scattering [32]. Investigating the effects of secondary interactions of heavy ion beams on lateral scattering remains important [36-39].

These studies provide important information that can be used to investigate the effect of lateral scattering in heavy ion radiotherapy. In this study, the contribution of the recoil interaction of heavy ions [40,41] to the total LET and its undesirable effects on the phonon production were investigated. In addition, as the atomic weight of heavy ions increases, they provide higher LET distribution on the target [34]. This provides possible clinical advantages for radiation-resistant tumors [26]. Optimal ion selection; was found to depend on tumor

[DOI: 10.52547/ijrr.21.1.18]

depth, dose levels, and contrast of radiosensitivity of the tumor and surrounding healthy tissues [42]. Similar to this study, it was presented that radiation-resistant healthy tissues were better protected with ^{4}He compared to heavy ions with a larger mass number of ^{4}He in radiosensitive tumors [42]. Like the water phantom used in this study, the water equivalent ratio of the investigated biomaterials was investigated with heavy ions. Thus, the effects of heavy ions on tissue equivalent biomaterials have increased their importance [43, 44]. Investigations of the effects of heavy ions not only on phantom interactions but also on DNA continue [45].

CONCLUSION

In the present study, Bragg curves, phonon curves, lateral straggle and recoils values of four different heavy ions with therapeutic energies were calculated by using MC TRIM simulation program considering the water phantom. The results obtained with these calculations were compared in a detailed manner. It is believed that this study will be used as a guide in determining the ion to be used in the treatment, since all interactions of the examined He, Li, Be and B heavy ions on the target were revealed in this study. Cancer treatment with heavy ion beams provides great advantages due to the different physical properties of heavy ions, high LET transfers and greater relative biological effectiveness. Thus, when it is dosed to deeply locate resistant tumors or "AVMs", it causes less toxicity in the surrounding healthy tissue. It is recommended and also planned as future work to repeat this simulation based experimental process by using other heavy ions, different phantoms and biomaterials.

ACKNOWLEDGMENTS

None.

***Ethics approval and consent to participate*:** Not applicable.

***Conflict of Interest*:** All authors declare no conflict of interest.

***Funding*:** None.

***Authors' contributions*:** All authors contributed equally to the design of the study, data collection and analysis, and the writing of the manuscript. All authors read and approved the final manuscript.

REFERENCES

1. Senirkentli GB, Ekinci F, Bostanci E, Güzel MS, Dağli Ö, *et al.* (2021) Therapy for Mandibula Plate Phantom. *Healthcare, **9**(2): 167*.
2. Ekinci F and Bölükdemir MH (2019) The Effect of the Second Peak formed in Biomaterials used in a Slab Head Phantom on the Proton Bragg Peak. *Journal of Polytechnıc, **23**(1): 129-136*.
3. Durante M and Loeffler JS (2010) Charged particles in radiation oncology Nature Reviews. *Clinical Oncology, **7**: 37–43, ISSN 1759-4774*.
4. PTCOG (2018) Particle therapy co-operative group. https:// www.ptcog.ch accessed: 2020-10-20
5. Tessonnier T, Böhlen TT, Ceruti F, Ferrari A, Sala P, (2017) Dosimetric verification in water of a Monte Carlo treatment planning tool for proton, helium, carbon and oxygen ion beams at the Heidelberg Ion Beam Therapy Center. *Physics in Medicine and Biology, **62** (16): 6579–6594*.
6. Tessonnier T, Mairani A, Brons S, Haberer T, Debus J, Parodi K (2017) Experimental dosimetric comparison of ^{1}H, ^{4}He, ^{12}C and ^{16}O scanned ion beams. *Physics in Medicine and Biology, **62**(10): 3958-3982*.
7. Hong L, Goitein M, Bucciolini M, Comiskey R, *et al.* (1970) A pencil beam algorithm for proton dose calculations. *Physics in Medicine and Biology, **41**(8): 1305–1330*.
8. Kozlowska WS, Böhlen TT, Cuccagna C, Ferrari A, *et al.* (2019) FLUKA particle therapy tool for Monte Carlo independent calculation of scanned proton and carbon ion beam therapy. *Physics in Medicine and Biology, **64**: 075012*.
9. Mein S, Choi K, Kopp B, Tessonnier T, Bauer J, *et al.* (2018) Fast robust dose calculation on GPU for high-precision 1H, 4He, 12C and 16O ion therapy: the FRoG platform. *Scientific Reports, **8**(1)*.
10. Lundkvist J, Ekman M, Ericsson S, Jonsson B, Glimelius B (2005) Proton therapy of cancer: Potential clinical advantages and cost-effectiveness. *Acta Oncol, **44**(8): 850–61*.
11. Kantemiris I, Karaiskos P, Papagiannis P, Angelopoulos A (2011) Dose and dose averaged LET comparison of H^{1}, He^{4}, Li^{6}, Be^{8}, B^{10}, C^{12}, N^{14} and O^{16} ion beams forming a spread-out Bragg peak. *Med Phys, **38**(12): 6585–91*.
12. Pshenichnov I, Mishustin I, Greiner W (2008) Comparative study of depth-dose distributions for beams of light and heavy nuclei in tissue-like media. *Nucl Instrum Methods B, **266**(7): 1094-1098*.
13. Tessonnier T, Mairani A, Chen W, Sala P, Cerutti F, *et al.* (2018) Proton and helium ion radiotherapy for meningioma tumors: a Monte Carlo-based treatment planning comparison. *Radiation Oncology, **13**(1)*.
14. Yabe T, Yamamoto S, Oda M, Mori K, Toshito T, Akagi T (2020) Prediction of dose distribution from luminescence image of water using a deep convolutional neural network for particle therapy. *Medical Physics, **47**(9): 3882-3891*.
15. Dudouet J, Cussol D, Durand D, Labalme M (2014) Benchmarking GEANT4 nuclear models for hadron therapy with 95 MeV/nucleon carbon ions. *Phys Rev C, **89**: 054616*.
16. Dokic I, Mairani A, Niklas M, Zimmermann F, Chaudhri N, *et al.* (2016) Next generation multi-scale biophysical characterization of high precision cancer particle radiotherapy using clinical proton, helium-, carbon- and oxygen ion beams. *Oncotarget, **7**(35): 56676-56689*.
17. Rogers D (2006) Fifty years of Monte Carlo simulations for medical. *Physics in Medicine and Biology, **51**: R287-R301*.
18. Ziegler JF, Biersack JP, Ziegler MD (2008) SRIM-The Stopping and Range of Ions in Matter; SRIM Co: Boston, MA, USA, 2008; ISBN 0-9654207-1-X.
19. Posselt M and Biersack JP (1986) Influence of recoil transport on energy-loss and damage profiles. *Nuclear Instruments and Methods in Physics Research B, **15**(1-6): 20-24*.
20. Behrens R and Hupe O (2016) Influence of the phantom shape (slab, cylınder or alderson) on the performance of an hp (3) eye dosemeter. *Radiation Protection Dosimetry, **168**(4): 441-449*.
21. Kinchin GH, Pease RS. 1955 The Displacement of Atoms in Solids by Radiation. *Rep Prog Phys, **18**: 1-51*.
22. Stoller R, Toloczko M, Was G, Certain A, Dwaraknath S, Garner F (2013) On the use of SRIM for computing radiation damage exposure. *Nucl Instrum Methods Phys Res B, **310**: 75-80*.
23. Khlifa RH, Nikitenkov NN, Viktor N, Kudiiarov VN (2021) On the use of chromium coating for inner-side fuel cladding protection: Thickness identification based on fission fragments implantation and damage profile. *Coatings, **11**(6): 710*.
24. Ziegler JF (2006) SRIM: The stopping and range of ion in matter. https://www.srim.org accessed: 20.09.2019
25. Golovchenko AN, Skvarč J, *et al.* (2002) Total charge-changing and partial cross-sectio measurements in the reactions of ~100-250 MeV/nucleon ^{12}C in carbon, paraffin and water. *Phys Rev C, **66**: 039901*.
26. Karger CP, Jakel O, Palmans H, Kanai T (2010) Dosimetry for ion beam radiotherapy. *Phys Med Biol, **55**: R193-R234*.
27. ICRU (1979) International Commission on Radiation Units and Measurements. Average Energy Required to Produce an Ion Pair, ICRU Report 31 (International Commission on Radiation Units and Measurements, Bethesda, MD)
28. Ekinci F, Bostanci E, Guzel MS, Dagli O (2022) Effect of different

[DOI: 10.52547/ijrr.21.1.18]

embolization materials on proton beam stereotactic radiosurgery Arteriovenous Malformation dose distributions using the Monte Carlo simulation code. *Journal of Radiation Research and Applied Sciences,* ***15****(3): 191-197*.
29. Loeffler JS and Durante M (2013) Charged particle therapyoptimization, challenges and future directions. *Nat Rev Clin Oncol,* ***10****: 411-424*.
30. Uhl M, Mattke M, Welzel T, Roeder F, Oelmann J, Habl G, *et al.* (2014) Highly effective treatment of skull base chordoma with carbon ion irradiation using a raster scan technique in 155 patients: first long-term results. *Cancer,* ***120****(21): 3410-3417*.
31. Schulz-Ertner D and Tsujii H (2007) Particle radiation therapy using proton and heavier ion beams. *J Clin Oncol,* ***25****(8): 953-964*.
32. Grun R, Friedrich T, Kramer M, Zink K, Durante M, *et al.* (2015) Assessment of potential advantages of relevant ions for particle therapy: a model-based study. *Med Phys,* ***42****(2): 1037-1047*.
33. Phillips TL, Fu KK, Curtis SB (1977) Tumor biology of helium and heavy ions. *Int J Radiat Oncol Biol Phys,* ***3****: 109-113*.
34. Strobele J, Schreiner T, Fuchs H, Georg D (2012) Comparison of basic features of proton and helium ion pencil beams in water using GATE. *Z Med Phys,* ***22****(3): 170-178*.
35. Orecchia R, Krengli M, Jereczek-Fossa BA, Franzetti S, Gerard JP. 2004. Clinical and research validity of hadrontherapy with ion beams. *Crit Rev Oncol Hematol,* ***51****(2): 81–90*.
36. Matsufuji N, Fukumara A, Komori M, Kanai T, Kohno T (2003) Influence of fragment reaction of relativistic heavy charged particles on heavy-ion radiotherapy. *Phys Med Biol,* ***48****(11): 1605-1623*.
37. Matsufuji N, Komori M, Sasaki H, Akiu K, Ogawa M, Fukumura A, *et al.* (2005) Spatial fragment distribution from a therapeutic pencil-like beam in water. Phys Med Biol, ***50****(14): 3393-3403*.
38. Gunzert-Marx K, Iwase H, Schardt D, Simon RS. 2008 Secondary beam fragments produced by 200 MeV u-1 12C ions in water and their dose contributions in carbon ion radiotherapy. *New J Phys,* ***10****: 075003*.
39. Haettner E, Iwase H, Krämer M, Kraft G, Schardt D. 2013 Experimental study of nuclear fragmentation of 200 and 400 MeV/n ^{12}C ions in water for applications in particle therapy. *Phys Med Biol,* ***58*** *(23): 8265-8279*.
40. Qi M, Yang Q, Chen X, Duan J, Yang L (2021) Fast calculation of mont carlo ion transport code. *Journal of Physics, Conference Series 1739, 012030*.
41. Ekinci F, Bostanci E, Dagli O, Guzel MS (2021) Analysis of Bragg Curve parameters and lateral straggle for proton and carbon beam. *Communications Faculty of Sciences University of Ankara Series A2-A3 Physical Sciences and Engineering,* ***63****(1): 32–41*.
42. Burigo L, Pshenichnov I, Mishustin I, Bleicher M (2015) Comparative study of dose distributions and cell survival fractions for 1H, 4He, 12C and 16O beams using Geant4 and Microdosimetric Kinetic model. *Phys Med Biol,* ***60****(8): 3313-31*.
43. Hajiloo N, Akbari M, Malekie S (2021) Evaluation of water equivalent ratio (WER) values for polyethylene, polymethyl methacrylate, polystyrene, lead, tungsten and aluminum at helium ion energies ranging from 25-250 MeV/u through Monte Carlo simulation. *Int J Radiat Res,* ***19****(3): 661-668*.
44. Bechchar R, Senhou N, ghassoun J (2019) A fast and accurate analytical method for 2D dose distribution calculation around brachytherapy sources in various tissue equivalent phantoms. *Int J Radiat Res,* ***17****(4): 531-540*.
45. Ahmadi Ganjeh Z, Eslami-Kalantari M, Ebrahimi Loushab M, Mowlavi A (2020) Investigation of the direct DNA damages irradiated by protons of different energies using geant4-DNA toolkit. *Int J Radiat Res,* ***18****(4): 809-815*.

[DOI: 10.52547/ijrr.21.1.18]